Measuring and Modifying the Spontaneous Emission Rate of Erbium near an Interface

E. Snoeks, A. Lagendijk, and A. Polman

FOM Institute for Atomic and Molecular Physics, Kruislaan 407, 1098 SJ Amsterdam, The Netherlands

(Received 3 October 1994)

Erbium implanted sodalime silicate glass was covered with a range of transparent liquids. The spontaneous emission rate of Er^{3+} around 1.54 μm shows clear changes depending on the liquid refractive index and Er depth. A rigorous quantum mechanical calculation shows that the effect of the interface on the spontaneous emission rate is fully described by the classical density of optical modes as a function of distance from the interface. The data provide the first direct determination of the radiative transition rate (45 s^{-1}) at 1.54 μm of Er^{3+} which is widely used in optical amplifiers.

PACS numbers: 42.50.Wm, 32.70.Fw, 68.55.Ln, 78.66.Jg

Spontaneous emission is interpreted as a consequence of interaction between matter and electromagnetic radiation. Previous experiments, using for instance Rydberg atoms or semiconductor structures, have demonstrated that spontaneous emission can be influenced in cavities or near mirrors [1–7]. In this Letter we will show an extremely simple way to modify the spontaneous emission rate, merely by bringing liquid films with certain refractive index in contact with a silica glass surface which is locally doped with luminescent Er^{3+} ions. Erbium shows clear photoluminescence (PL) around 1.54 μm [8], an important wavelength in optical telecommunication [9].

The theoretical description of spontaneous emission is usually based on concepts from quantum electrodynamics such as vacuum fluctuations and a creation and annihilation formalism. The inclusion of a dielectric interface requires special attention [10]. In this case, the variation in the spontaneous emission rate can be accounted for by the local classical density of states (DOS), which appears in Fermi's golden rule. In this Letter, a straightforward calculation of the local DOS is performed, given the Fresnel equations for transmission and refraction at a dielectric interface. The analysis describes our data on the modification of the spontaneous emission rate as a function of refractive index, and serves to determine for the first time the radiative lifetime of Er in silicate glass, a parameter of great importance for Er-doped optical gain materials in telecommunication technology.

Two samples of bulk sodalime silicate glass (refractive index $n_0 = 1.5$) were implanted with 500 keV Er ions. Sample A was covered with a 120 nm thick Al film as a stopping layer, and sample B was uncovered during implantation. After implantation, the Al layer was etched off, and a thermal anneal at 512 °C was performed. Erbium depth profiles for both samples, as determined using 2 MeV $^4He^+$ Rutherford backscattering spectrometry (RBS), are shown in Fig. 1. The open data points for sample A show a profile peaked at the glass surface, with a half-width of 70 nm. The measured profile is a convolution of the detection resolution and the actual profile which is discontinuous at the surface. The drawn line

shows the deconvoluted profile, which has a surface concentration of ~ 0.25 at. %. The solid data points in Fig. 1 show a Gaussian profile for sample B, centered at 150 nm depth from the surface, where the Er concentration is 0.17 at. %. The full width at half maximum is 100 nm. PL spectroscopy was carried out at room temperature. The 514.5 nm line of an Ar-ion laser was used to excite the Er, and the luminescence was spectrally analyzed with a monochromator and detected with a liquid-nitrogen cooled Ge detector. PL decay measurements were performed after exciting with a 1.5 ms pulse, using a digital averaging oscilloscope. Further details on sample preparation and PL measurements can be found in Ref. [11]. Various liquids, with refractive indices ranging from 1.3 to 1.7, and thickness in the order of a mm, were brought in contact with the sample surface on the front, while the luminescence signal was collected on the back side (see inset in Fig. 2).

Clear PL around 1.54 μm, characteristic [8] for the $^4I_{13/2} \rightarrow {}^4I_{15/2}$ intra-$4f$ transition of Er^{3+}, is observed [11] in both samples A and B. Figure 2 shows the PL
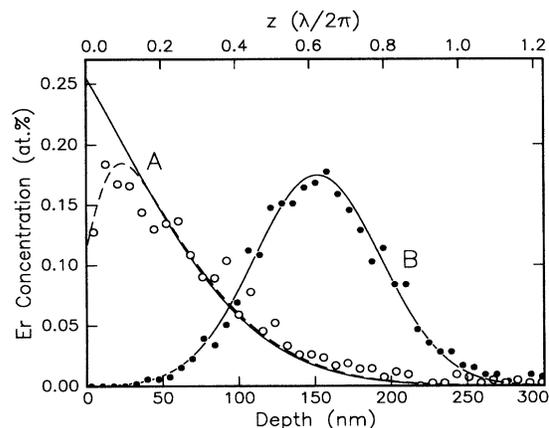

FIG. 1. Erbium concentration profiles as determined with RBS (open and solid data points). The drawn lines are deconvoluted for the detection resolution. The top axis shows the distance in units of $\lambda/2\pi$ (where $\lambda = 1.537$ μm is the spontaneous emission wavelength in vacuum).
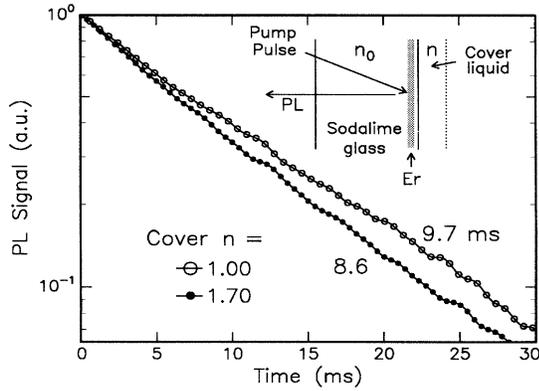
FIG. 2. PL decay traces of the 1.537 μm emission from sample A on a logarithmic scale. The solid data points were measured with a methylene-iodide film ($n = 1.70$) covering the surface, the open data points in air. The inset shows how the luminescence signal was collected at the back of the sample, while the Er-doped front side was covered with various liquids with index n.
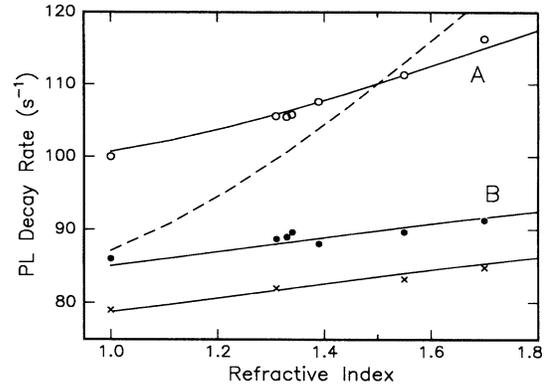

FIG. 3. Measured PL decay rates as a function of refractive index n of the cover liquids. The index of the sodalime glass is $n_0 = 1.50$. Data are shown for both samples A (open data points) and B (solid data points). The × symbols represent data from sample B measured one year later. The solid lines are calculations using Eq. (8); the dashed line shows a calculation assuming only radiative decay.

decay measured around 1.537 μm for sample A in air (open data points). A single exponential decay with a $1/e$ decay time of 9.7 ms is found. The curve marked by solid data points in Fig. 2 shows the PL decay when a film of methylene-iodide with refractive index of $n = 1.70$ is brought in contact with the glass surface. In this case a $1/e$ time of 8.6 ms is observed, a reduction by 13%. After the surface was cleaned again, the $1/e$ time returned to 9.7 ms. Additional measurements were performed, using other liquids with different refractive indices in the range 1.3–1.7. PL decay rates were defined from the data by inverting the $1/e$ decay times. These are shown in Fig. 3 as open data points, together with the data measured on sample B (solid points), which has a deeper Er profile. Also for this sample an increase of the PL decay rate is observed as a function of the refractive index of the cover liquid, but the effect is smaller than for sample A. These measurements provide an extremely simple demonstration of modification of the PL decay rate by varying the optical surrounding. The effect is strongest for high refractive index contrasts, and Er profiles close to the surface.

In the dipole approximation the coupling between an atom and the electromagnetic radiation field is given by

$$\mathcal{H}_{int} = -\hat{\mu}(\mathbf{R}) \cdot \hat{\mathbf{E}}(\mathbf{R}), \tag{1}$$

where $\hat{\mu}(\mathbf{R})$ is the dipole moment operator of the atom positioned at $\mathbf{R}$ and $\hat{\mathbf{E}}(\mathbf{R})$ is the electric field operator. The spontaneous emission rate is given by Fermi's golden rule

$$W(\mathbf{R}) = \frac{2\pi}{\hbar^2} |\langle f|\mathcal{H}_{int}|i\rangle|^2 \delta(\omega_i - \omega_f), \tag{2}$$

in which $|i\rangle$ and $|f\rangle$ are the initial and final states with energies $\hbar\omega_{i,f}$. First we look at the ith Cartesian

component of the electric field:

$$W_i(\mathbf{R}) = \frac{2\pi}{\hbar^2} |\langle a|\hat{\mu}_i|b\rangle|^2$$
$$\times \sum_{\{\ell\}} \langle 0|\hat{E}_i(\mathbf{R})^\dagger|\ell\rangle \langle \ell|\hat{E}_i(\mathbf{R})|0\rangle \delta(\omega - \omega_\ell), \tag{3}$$

where $|a\rangle$ and $|b\rangle$ denote the ground state and excited state of the atom separated by energy $\hbar\omega$, and $|0\rangle$ and $|\ell\rangle$ the initial and final states of the field separated by energy $\hbar\omega_\ell$. The field operator consists of creation operators and an expansion in normalized eigenvectors of the geometry. We use

$$\hat{E}_i(\mathbf{R}) = \sum_\lambda \{[\hbar\omega_\lambda/2\varepsilon(\mathbf{R})]^{1/2}$$
$$\times [ia_\lambda^\dagger \varphi_{\lambda,i}(\mathbf{R}) \exp(-i\omega_\lambda t) + \text{H.c.}]\}, \tag{4}$$

in which $\varphi_{\lambda,i}(\mathbf{R})$ is ith Cartesian component of the λth normalized eigensolution of the classical Maxwell wave equation. Insertion of Eq. (4) into Eq. (3) using the commutation rules for the creation and annihilation operators gives

$$W_i(\mathbf{R}) = \frac{\pi\omega}{\hbar\varepsilon(\mathbf{R})} |\langle b|\hat{\mu}_i|a\rangle|^2 \rho_i(\omega, \mathbf{R}), \tag{5}$$

with

$$\rho_i(\omega, \mathbf{r}) \equiv 2\omega \sum_\lambda \varphi_{\lambda,i}(\mathbf{r}) \delta(\omega^2 - \omega_\lambda^2) \varphi_{\lambda,i}(\mathbf{r}). \tag{6}$$

Here, $\rho_i(\omega, \mathbf{r})$ is the ith contribution to a local classical DOS [12]

$$\rho(\omega, \mathbf{r}) \equiv \sum_i \rho_i(\omega, \mathbf{r}). \tag{7}$$

For an absolute determination of $W(\mathbf{R})$ the field operator

in Eq. (1) should be used for the local field. From dielectric theory it is well known that the local field seen by an atom is not the same as the macroscopic field. Since the local field is due to the microscopic environment around the atom, it is not influenced by the liquid films that are applied in our experiment. Thus, the only parameter that is varied in our experiment is the macroscopic $\rho(\omega, \mathbf{r})$.

The classical DOS [Eq. (6)] can be calculated numerically to any desired precision. For this calculation the complete set of incoming plane waves with one single frequency is summed, using reflection and refraction as given by the Fresnel coefficients. For our problem only the isotropic combination of directions and polarizations is relevant, because the Er ions are randomly distributed in the glass matrix.

Figure 4 shows the result of this calculation of the classical density of optical modes, as a function of the distance from an interface, where the refractive index steps from n_0 to n. The density $f_{1.5}$ is normalized to 1 for a bulk material with refractive index $n_0 = 1.5$. Two cases are shown: In one case the index steps from 1.5 to 1.0 at the interface, and in the other case from 1.5 to 3.0. The distance is given in units of $\lambda/2\pi$, where λ is the emission wavelength in vacuum. As can be seen, the DOS is discontinuous at a dielectric interface. This discontinuity is caused by the polarization component parallel to the interface. The oscillations on either side of the interface have a periodicity of $\lambda/2n$ and are due to interference between incoming and reflecting waves. For large distances away from the interface the DOS is proportional to the refractive index. This classical DOS also determines the vacuum field fluctuations: Fig. 4 indeed agrees with the result of a recent calculation of vacuum-field fluctuations [10].

The factor $f_{1.5}(n, z)$ from Fig. 4 determines the radiative decay rate for Er at distance z from the interface when

a liquid with refractive index n covers the glass, relative to the rate in bulk sodalime glass. The distance z is integrated out by weighted averaging over the Er concentration profile from Fig. 1. In addition to radiative decay, Er may show nonradiative decay, which is not sensitive to changes in the optical DOS. Therefore the total PL decay rate may be written as

$$W_{\text{tot}}(n) = W_{\text{nr}} + f_{1.5}(n)W_r, \qquad (8)$$

where W_{nr} is the nonradiative decay rate, and W_r the radiative rate in absence of the interface ($n = 1.5$).

The dashed line in Fig. 3 shows the result of a calculation of $W(n)$ using $W_{\text{nr}} = 0$ and $W_r = 110$ s^{-1} for sample A. As can be seen, the measured data show a much smaller dependence on n than the calculation. Therefore a nonradiative component has to be introduced: The solid line is obtained using $W_r = 45$ s^{-1} and $W_{\text{nr}} = 65$ s^{-1}. As can be seen, this describes the data quite well. The PL efficiency for this sample is $W_r/(W_r + W_{\text{nr}}) = 0.41$. A similar calculation for the data for sample B, with the deeper Er profile, is also shown in Fig. 3. The radiative rate again is found to be 45 s^{-1}, indicating that the calculated z dependence of the DOS agrees with the experimentally observed depth dependence. The nonradiative decay rate in this case is 45 s^{-1}, slightly lower than for sample A. This is explained by the fact that the Er concentration in sample A is higher than in sample B, resulting in concentration quenching which increases W_{nr} [11,13]. In addition, there may be quenching centrally related to the surface.

These data provide the first experimental determination of the radiative lifetime and quantum efficiency of the optical transition of Er^{3+} at 1.54 μm which is important in modern optoelectronic devices. Other attempts to determine these parameters have failed. For instance, because the multiphonon relaxation rate of the $^4I_{13/2}$ manifold is negligible because of the relatively low phonon energies in silica, the quantum efficiency cannot be determined from the temperature dependence of PL decay [14,15]. Theoretical estimates of the radiative decay rate, using Judd-Ofelt theory [8] to determine the matrix elements $\langle a|\hat{\mu}|b\rangle$ in Eq. (5), may yield uncertainties of up to 100%, in addition to the fact that the local-field correction has to be evaluated. The nonradiative decay found in the present work is attributed to coupling to acceptor states in the host such as impurities (hydroxyl groups, iron) and structural defects, possibly to some extent introduced by the ion beam during the implantation process [11].

As an interesting sidetrack, we show how the method used in this Letter can in fact be used to study structural defects in the silica network. The PL decay measurements using cover liquids were repeated in sample B one year after the first experiment. The results are included in Fig. 3 with × symbols. As can be seen, the emission rates over the entire index range decreased by 6 s^{-1}. A freshly produced sample still reproduced the original data.
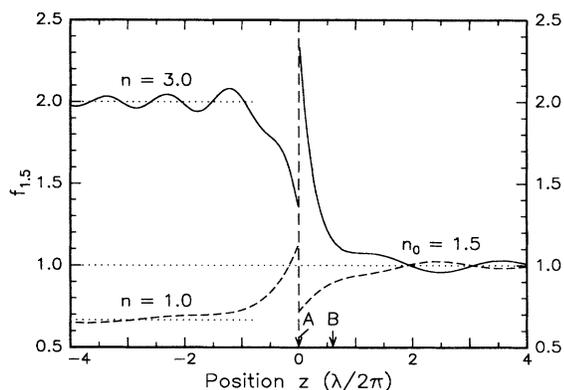

FIG. 4. Polarization- and angle-averaged local classical density of optical modes, on both sides of an interface between infinite half-widths. The refractive index on one side is $n_0 = 1.50$. Calculations are shown for $n = 1.00$ and 3.00 on the other side. The arrows indicate the locations of the Er profiles.

The slope of the calculated curve through the $\times$ data is identical to the slope of the filled circles, indicating that W_r is unchanged, whereas the downward shift of the curve indicates a decrease in W_{nr}. This is explained by annihilation of ion-beam induced defects that quench the luminscence. Indeed it is known that such structural relaxation processes in glasses can occur over very long time scales.

In conclusion, we have demonstrated that the spontaneous emission rate at 1.54 μm of Er^{3+} in glass can be modified simply by applying liquids on the surface. We show theoretically that the changes in the spontaneous emission rate can be fully described by changes in the local classical DOS. By comparing the calculated DOS with the measured decay rates, we were able to distinguish radiative and nonradiative decay components in the luminescence of Er^{3+}.

The measurements and calculations in this Letter may impact several fields. The notion that although the PL lifetime of Er in sodalime glass is relatively long (11 ms), the purely radiative lifetime is twice as high, has implications for the design of Er-based lasers and optical amplifiers in silica fibers and planar waveguides [9]. The local DOS also affects the cross sections for stimulated emission. Furthermore, in view of the simplicity of the measurement and the analysis reported here, it becomes possible to study spontaneous emission and nonradiative quenching of other luminescent ions in other materials as well.

[1] A. M. Vredenberg, N. E. J. Hunt, E. F. Schubert, D. C. Jacobson, J. M. Poate, and G. J. Zydzik, Phys. Rev. Lett. **71**, 517 (1993).
[2] R. G. Hulet, E. S. Hilfer, and D. Kleppner, Phys. Rev. Lett. **55**, 2137 (1985).
[3] D. J. Heinzen, J. J. Childs, J. E. Thomas, and M. S. Feld, Phys. Rev. Lett. **58**, 1320 (1987).
[4] F. De Martini, G. Innocenti, G. R. Jacobovitz, and P. Mataloni, Phys. Rev. Lett. **59**, 2955 (1987).
[5] K. H. Drexhage, J. Lumin. **12**, 693 (1970).
[6] Z. Huang, C. C. Lin, and D. G. Deppe, IEEE J. Quantum Electron. **29**, 2940 (1993).
[7] E. Yablonovitch, T. J. Gmitter, and R. Bhat, Phys. Rev. Lett. **61**, 2546 (1988).
[8] S. Hüfner, *Optical Spectra of Transparent Rare-Earth Compounds* (Academic, New York, 1978).
[9] E. Desurvire, Phys. Today **47**, No. 1, 20 (1994).
[10] H. Khosravi and R. Loudon, Proc. R. Soc. London A **433**, 337 (1991).
[11] E. Snoeks, G. N. van den Hoven, and A. Polman, J. Appl. Phys. **73**, 8179 (1993).
[12] B. A. van Tiggelen and E. Kogan, Phys. Rev. A **49**, 708 (1994).
[13] J. C. Wright, in *Radiationless Processes in Molecules and Condensed Phases,* edited by F. K. Fong (Springer, Heidelberg, 1976), Chap. 4.
[14] W. Ryba-Romanowski, J. Lumin. **46**, 163 (1990).
[15] J. M. Flaherty and B. Di Bartolo, J. Lumin. **8**, 51 (1973).